Mapping of Floodplains in the Atankwidi River Basin

LUNDS TEKNISKA HÖGSKOLA
Lunds universitet

TU Delft
Delft University of Technology

IWMI
International Water Management Institute

Master's Thesis Andrej Nikolaev
Lund Institute of Technology
2009-02-28

Modeling and mapping of floodplains in the Atankwidi river basin

Examiner:
Magnus Persson

Opponent:
Marion Guegan

Supervisor:
Lars Bengtsson

Written by:
Andrej Nikolaev

MSc Thesis final report
Lund, February 2010

Lund Institute of Technology
Delft University of Technology
IWMI

Preference

This report is the final thesis for the master in Civil Engineering at Lund Institute of Technology, Sweden. The subject of study for this thesis is the flood spread in the Atankwidi River Basin, which is situated in the Upper East Region of Ghana. The objective is to produce a flood map of the 2007 and 2009 floods over the Atankwidi River Basin. By being able to compare places where the floodplains usually occur with places which in the following dry-season yield a good quantity of water it is possible to verify if there is an interconnection between the floodplains and the shallow groundwater aquifers.

The project was conducted in collaboration with TU Delft University in Holland and IWMI in Ghana. The research included a two months field work in Ghana, preparation work and an aftermath of about 5 months in Delft and Lund.

I would like to thank especially much my supervisor in TU Delft Professor Nick van de Giesen for giving me the opportunity to work on such an exciting project and for helping and guiding me through it. Thanks also to Martine Poolman for all the support concerning the trip to Ghana and Olivier Hoes for the help with the ArcGIS and SOBEK softwares.

I would also like to thank my home University and especially Professor Lars Bengtsson for his calm and gentle guidance.

Also a big thank you to Dr. Boubacar Barry for looking after me in Ghana. The field assistant Jacob, without whom I would have been completely lost and the driver Salisu for the help with local guidance and other logistical issues.

Wish you a happy reading

Lund, January 2010

Andrej Nikolaev

Summary

The Upper East Region of Ghana is situated in a semi-arid region with a distinct dry- and rainy-period. The average annual precipitation during the rainy period – April to September – is around 1000 mm with peak downfall around august. This concentrated precipitation often creates problems in terms of big floods, leading to destruction of property and crops.
The UER is considered to be one of the least economically developed regions in the whole of the Volta Basin, depending on a very large extent on its agricultural production, thus a destruction of crops due to flooding often implies serious economical and social hardships for all the people living in the area.
Floods in the UER are, however, not only a menace to lives and livelihoods in the UER but it is also provides the basis of food and income. The Shallow Groundwater Irrigation conducted during the dry season is considered by many to have a direct link to the floodplains – recharging the groundwater locally. Rice, commonly grown in the region is another example of a crop demanding to be flooded in order to give a good harvest.

The use of remote sensing satellite imagery – especially radar – has recent times more and more been proven an effective tool in floodplain mapping. The main problem with only using satellite images in the mapping procedure is that images are only taken at a specific time – dependent on the passing time of the satellite – hence sometimes missing the time when the flood is at its peak.

In order to be able to compensate for this insufficiency one can seek assistance in 2D flood spread modeling using some of the adequate softwares, i.e. Lisflood or SOBEK.
SOBEK-rural has been chosen for this project.
By modeling flood spread over a digital elevation model one is able to withdraw information on the areas which were most likely to be flooded during the specific flood event.

Combining the information from the satellite images and from the modeling of the DEM it is possible to give a more accurate estimation of the flood spread during its peak.

The DEM used for this project was downloaded from the USGS Hydrosheds and provided a resolution of about 96 meters.
The satellite images used where C- and L-band images taken from ESA and JAXA respectively. The resolution of the images were 12.5 meters and were chosen to best be able to capture the year 2007 – the year of one of the biggest floods to ever hit the UER – and 2009 – the year when the fieldwork was conducted.

The multi-temporal satellite data together with the SOBEK-modeled DEM proved to be a good combination for the project and gave a rough estimation as to where the floodplains probably would occur during its peak. A DEM of much higher resolution is required to produce an accurate map – the 96 meter resolution DEM proved to be insufficient in

giving the satellite images any accurate support, but rather served as e rough indication tool of the flood trends. Also the ASAR satellite images proved to be too noisy to give any relevant flooding information.

The results showed on the complicated nature of the basin where it seemed like that due to its flatness the floodplains became very widely spread ponding in the micro sub-basins. This trend was thought not to be seen on the modeling of the DEM because to its rough resolution.

Due to the problems encountered with the ASAR images, the roughness of the DEM and the absence of flood during the fieldwork, the results from this project can only serve as a rough indicator of the common flood zones that are thought to have dominated in their prominence and extent the floodplains during the 2007 flood. No map was made for 2009 because of the absence of clear floodplains that year.

The final map is obtained by comparing the Idrisi-mapped satellite images and the SOBEK-modeled DEM, mapping out the most prominent and large flooded areas. This final map is well suited for determining whether there is a relationship between the floodplains and the shallow ground water recharge; this by seeing if the places were floods occurred indeed gave good yield for the SGW-wells the following dry-season.

Table of contents

Table of figures

Table of Tables

List of abbreviations and explanation of terms

DEM – Digital Elevation Model
UER – Upper East Region
ASAR – Advanced Synthetic Aperture Radar
SGI – Shallow Groundwater Irrigation
RMS-Error – Root Mean Square Error
MINDIST – Minimum Distance to Mean, mapping algorithm
IWMI – International Water Management Institute

1. Introduction

In August 2007 during one of its rainy seasons the Upper East Region in Ghana experienced one of the most devastating floods which have ever been recorded in the region, destroying houses and livelihoods for hundreds of thousands of people. According to the BBC (2007) the number of affected people in the whole of northern Ghana was estimated to 400'000 and 20 people dead. Even though this was an extreme event, the people living in the UER face every now and then big hardships due to flood devastation.
The flooding, however, is not a completely undesirable phenomenon with which the farmers have to deal. Crops like rice are for example big water users and need to be flooded in order to produce a good harvest.
Another use of the rainy season floodplains can be found in the dry season agriculture. The vast potential of Shallow Groundwater Irrigation (SGI) has recently been discovered by the farmers (Berg, 2008). The SGI is conducted in the dry season, mostly for growing tomatoes – because of their low water need – and is practiced by digging shallow wells and from there extracting the water. The SGI is a highly laborious task, the wells do not always give good yield and the construction of the wells is to a high degree based on trial and error. There is potent theory that the shallow groundwater wells are mainly and directly recharged by water from floodplains dating from the previous rainy season – which explains the fact that the SGI is much more productive after a very wet year then after a dry one.
The by far largest economic activity in the UER is agriculture, which means that the economy and wellbeing of the region is very much affected by its natural climate – i.e. drought, flood, etc. – making its inhabitants extra sensitive to the whims of nature. With this all said one can see the importance and the potential in understanding the dynamics of the flood spread.

1.1 Objective

"*Map the floodplains of the 2007 and 2009 floods*"

Thus this project aims purely at investigating the 2D flood spread during the years 2007 and 2009. The reasons for choosing 2007 and 2009 as the years of study are that in 2007 a very large flood struck the area and 2009 was the year when the fieldwork was conducted.
Mapping the flood spread can in turn can help us understand the mechanisms behind the shallow ground water recharge.

1.2 Research strategy

To be able to map the 2009 and 2009 floodplains a 2D mapping of satellite images and computer modeling of the floodplains have been undertaken. All of the below mentioned information about the research strategy will be discussed in more detail in the chapters describing the actual implementation of the strategy. This chapter is only aimed at orientating and introducing the reader to the initial thought process.

1.2.1 Modeling

The modeling was done with the aid of the Dutch modeling software SOBEK RURAL 2.12.001, which is a commercial software (see: http://delftsoftware.wldelft.nl/), the software is developed by Deltares in collaboration with TU Delft. It is used here to simulate flooding over a USGS Hydrosheds Digital Elevation Model of Atenkwidi River Basin. The DEM is flooded by systematically placed flood nodes. The details behind the modeling procedure and the model are discussed in chapter 4 "floodplain modeling".

1.2.2 Mapping

The mapping was done based on L- and C-band radar, ALOS PALSAR & the Envisat ASAR respectively. The images have a spatial resolution of 12.5 m.
The mapping software used for the project was mainly Idrisi Andes but also some ArcGIS was used during the project. The mapping is discussed in greater detail in chapter 5 on mapping and the dates of the different images used can be seen in appendix A.

1.2.3 Modeling & Mapping

One of the reasons for both modeling and mapping the area is to make a more thorough investigation by, so to say, approaching the problem from two different angles. But the most important reason is the time dependency of the 2D flood spread and the brief moment during which the satellite images are taken, makes it very difficult to discuss the flood peak.
By comparing the flooded DEM with the mapped radar images it is possible to better assess the true peak of the flood spread.

1.2.4 Field work

The field work was conducted using a GPS to map the flooding and the different surfaces of the basin. Mapping the floodplains are necessary to be able to conduct an error analysis of the map to be created, this is done by comparing the mapped floodplaines with the actual floodplains recorded with the GPS – also known as ground-truth data. It is also necessary to map other parts of the basin to see which areas give which type of reflectance on the radar images. The river was also mapped using a small rubber boat and the GPS; this was done for orientation purposes, to clearly see where the river is flowing. Besides the GPS and the rubber boat, a motorcycle was used to get by in the basin and to get to the basin.

2. Area description

Ghana has – according to the CIA World Fact Book (2009) – a population of roughly 23.9 million. The country is made up of ten regions, the Upper East Regoin being one of them.
The UER of Ghana is the poorest and the most densely populated area in the whole of the Volta River basin (Schiffer et. al, 2008). The region is divided into six districts: Bawku East, Bawku West, Bongo, Builsa, Kassena-Nankana and Bolgatanga. The UER with its population of 917'000 covers 7.8% of Ghanas total landmass. The region is the gateway from Ghana to Burkina Faso and has always had a traditional importance as a trade route; the region was a part of the trans-Saharan trade routes, dating back thousands of years. (Ghana High Commission, 2010).
The Atankwidi River Basin, which is the area of this study, is situated in the Kassena-Nankana district of the UER between two cities, Navrongo – the administrative capital of the Kassena-Nankana district – and Bolgatanga – the administrative capital of the Bolgatanga district.
This section will go through the most relevant information about the Atankwidi River Basin and some of its surroundings, discussing the region's: geography, climate, and agriculture.

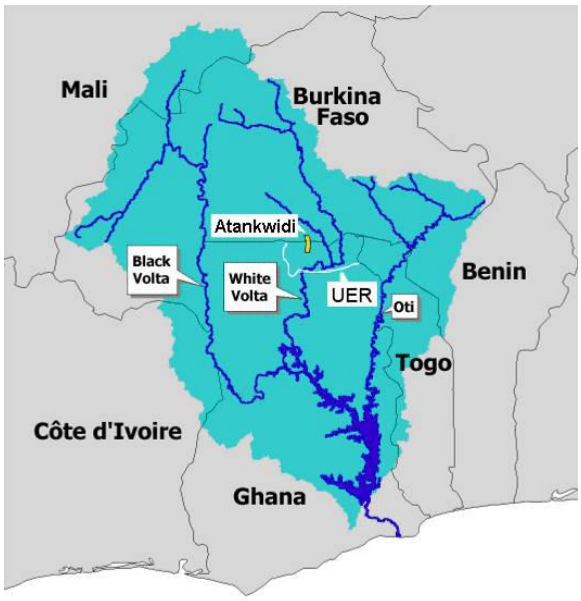

Figure 1 the Volta River Basin, with the tree main rivers, the White Volta, the Black Volta and the Oti River. The Atankwidi river basin is marked yellow on the image.

2.1 Geograhpy

The Atankwidi river basin is a small river basin – approximately 275 km^2 – situated in the Upper East Region of Ghana. The basin is however not entirely contained within the borders of Ghana; its northern part is in the territory of Burkina Faso (figure 2).

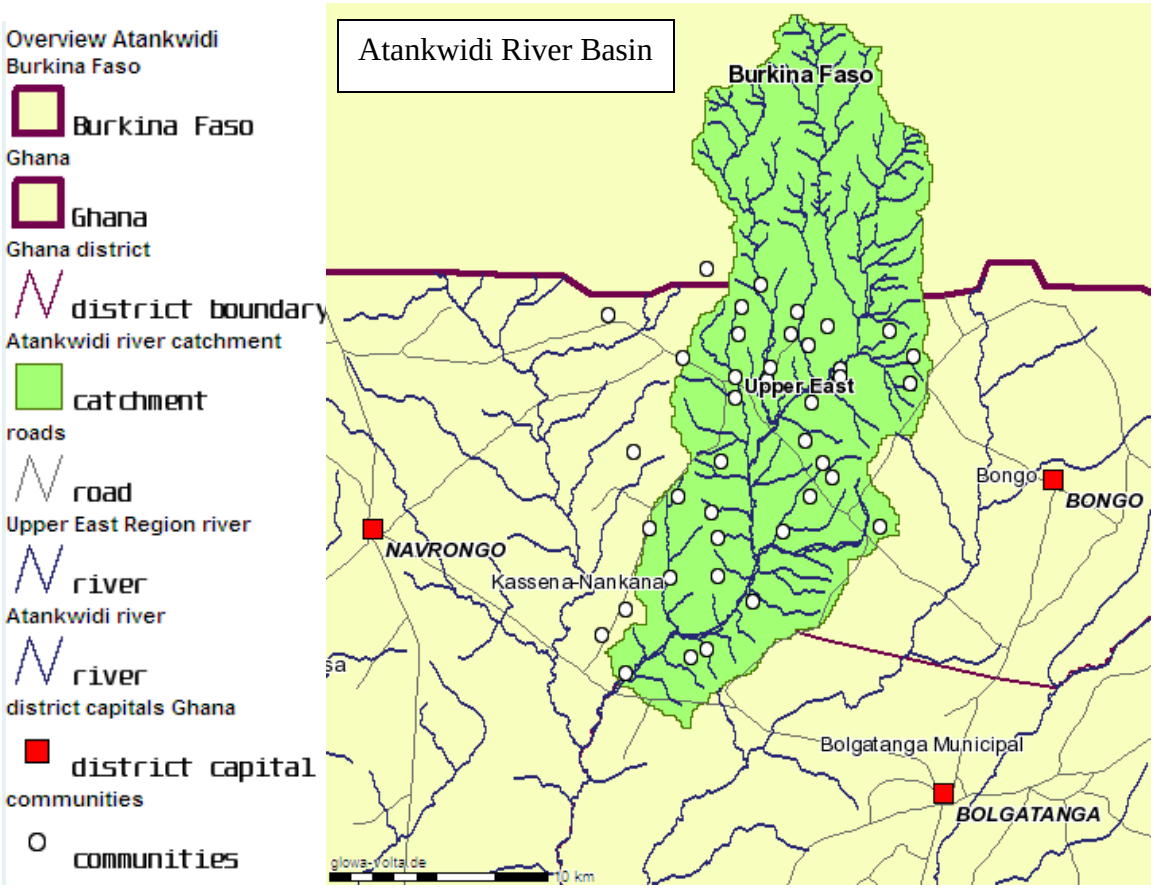

Figure 2 the Atankwidi River Basin with Burkina Faso in the north and Ghana Upper East Region south and the two citys Navrongo and Bolgatanga.

The basin is a small sub basin in the much larger Volta river basin (figure 1). The Atankwidi river serves a tributary to the White Volta River.

2.2 Climate

The climate in the basin is semi-arid with one rainy season – extending from April to September – and one dry season – going on from October to April. Figure 3 shows the ruling precipitation and temperature averages of the area, the meteorological data is here taken from Navrongo – a city situated ten kilometers west of the basin.

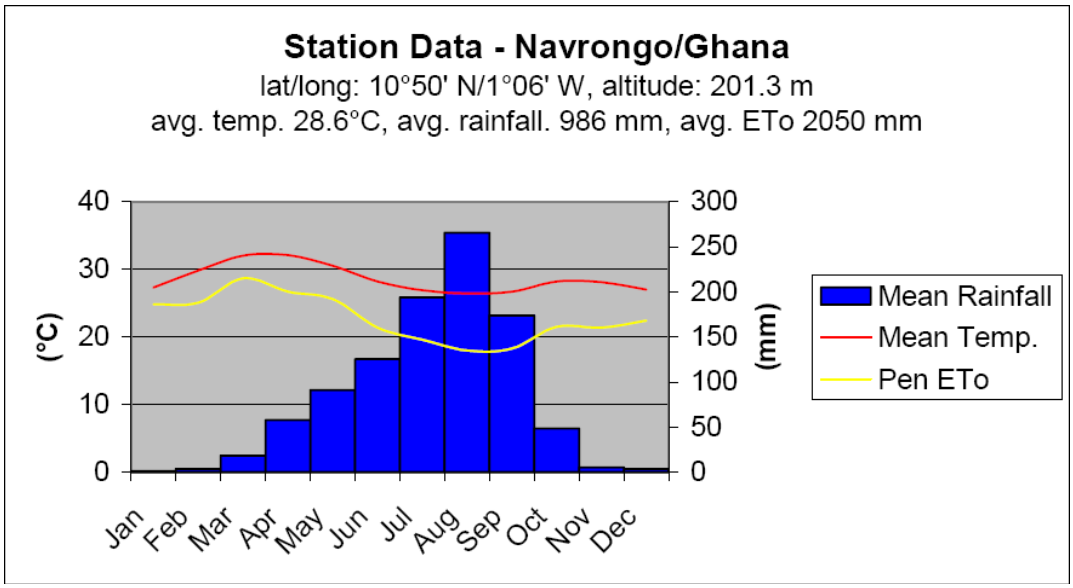

Figure 3 the average yearly precipitation and temperature data, taken from a measuring station in Navrongo.

As can be deduced from figure 3, the peak precipitation occurs often during the month of August and diminishes very fast ending already at the end of October.

2.3 Geology

The soil in the Atankwidi River Basin is quite clayey. Table 1 show an unpublished survey done by Fosu (2004), taken from the master's thesis of Berg (2008). The survey was done at Nyankpala, 10km west of Atankwidi.

Table 1 Soil survey near Navrongo. The soil textures are expressed as percentages represented in the 320 soil samples taken during the survey. (Fosu, unpublished data 2004)

Texture	*K_{sat} (m/d)*	*Bulk density (kg/m^3)*	*Porosity (%)*	*Soil type*
Clay loam (1.7%)	0.034	1660	37.4	Fluvisol
Loam (2.3%)	0.43	1760	33.6	Fluvisol
Loamy sand (25%)	1.18	1720	35.1	Leptosol
Sand (4%)	2.04	1840	30.6	Leptosol
Sandy clay (1.1%)	0.39	1860	29.8	Leptosol
Sandy clay loam (10.8%)	0.75	1790	32.5	Leptosol
Sandy loam (55.1%)	0.61	1730	34.7	Lixisol

The survey included 320 soil profile samples, the samples were taken at a depth of 0.3 to 0.45 m. The large presence of clay in the soil implies quite low infiltration rates and high surface runoff in case of heavy rains.

2.5 Agriculture

The by far largest and most important economical activity in the UER in general and in the Atankwidi basin especially is agriculture.
The agriculture in the Atankwidi can be divided into two categories carachterized by the type of crops grown, and specialized by the season, namely: dry season agriculture and rainy season agriculture. Those two are described in the subchapters below.

2.5.1 Rainy season agriculture

In the Atankwidi the rainy season agriculture is completely rain-fed and three dominating crops can be distinguished, namely: millet, rice and groundnut.
The rice needs a lot of water and is thus grown in regions that are prone to flooding, i.e. lowlands that are close to rivers or which are getting sufficient amount of runoff to flood the plants. Figure 4 below show a rice field, notice also the flatness of the basin.

Figure 4 a larger rice field about 400 m away from the Atankwidi River. The rice fields are in general situated some distance away from the river banks.

The millet needs water but does should not be flooded in it and is thus grown on high lands, especially along the rivers and around houses.

Figure 5 a millet field on the banks of the Atankwidi River. A very common site along the course of the river.

Figures 5 & 6, show the typical location of millet fields. The river banks rarely get flooded for a longer time period and are thus perfect for millet plantation. Houses are generally built in uplands and also provide a naturally convenient place for growing millet.

Figure 6 millet field around a farming community, provedes some shelter for the villagers and minimizes the distance to field.

The groundnut does not need much water at all and is grown only on the high land some distance from the Atankwidi River; figure 7 shows a typical groundnut field.

Figure 7 a large groundnut field surrounding an old Baobab tree.

There are also other types of crops grown in the basin during the rainy season, crops like: garden eggs, pepper are also popular but are not at all grown in the same extent as the three above mentioned crops, which completely dominate the whole landscape of the basin.

2.5.2 Dry season agriculture

During the dry season there is no rain-fed agriculture, the water is gathered from the ground by digging shallow wells, this procedure is known as Shallow Groundwater Irrigation (Berg, 2008)
The dry season agriculture is even more monotone then the rainy season agriculture when it comes to the number of different crops grown. The absolutely predominating crop cultivated during the dry season is the tomato (Berg, 2008). The tomato is chosen for the simple reason that it doesn't require a lot of water and it is also an important ingredient in the local cuisine.

Figure 8 tomato-farming to the left and to the right a hand-dug irrigation well (Berg, 2008)

Figure 8 shows a tomato-farming underway and to the right of that image is a hand-dug well that is used to irrigate the crops. Digging the wells is a very laborious activity given the tough nature of dry clay, the high temperature during the dry season and the fact that new wells must be dug not only every new dry season but also during the ongoing dry season due to shortages in water yield. The wells dug can have a depth reaching up to 6m (Berg, 2008).

2.6 Hydrology

The Atankwidi River has a cross section width of around 30-35 meters and a depth of around 3 m when completely full. Figure 9 shows a relatively full cross section of the Atankwidi River, the picture is taken in August.

Figure 9 the Atankwidi River

The river reacts fast to precipitation over the basin. It can almost be overflowing one day and have a very low water level on the following – i.e. if no rain is added during the period. The flatness of the area produces only a small slope, as a rough estimate the slope rarely reaches beyond 0.001 m/m. This should produce, during the peak of a flood, a water flow of maximum 200 m^3/s. An avarege flow during the peak of the rainy season could be around 35 m^3/s.

The floodplains occur throughout the river basin but they stay much longer in the southern part because of the draining function of the basin
The basin contains lot of small reservoirs but there are no large-scale water-regulators in the Atankwidi.
The Atankwidi River is a tributary to the much larger White Volta River. Upstream on the Burkina part of the Volta Basin, the White Volta is dammed by the Bagré Dam. Big floods usually occur in the Atankwidi Basin when the downstream water levels in the White Volta increase due to high releases of water from the Bagré Dam making it harder to drain the water from the Atankwidi.

3. Fieldwork

Conducting a fieldwork on site was a vital part of the project. The fieldwork consisted of a collection of ground truth data, using a GPS. The reason for the fieldwork was partly making an accuracy assessment of the mapping and partly to get generally acquainted with the research area. The aim of this chapter is to describe the underlying idea behind the fieldwork, the fieldwork itself and the outcome.

3.1 Reason for the fieldwork

The L- and C-band maps are not very clear due to their large wave lengths hence some foreknowledge of the site is recommended in order to be able to make a reasonably good-quality map. The second reason for going through with the fieldwork is to be able to conduct an error analysis of the created maps.
The error analysis involves comparing the ground truth data – i.e. the area mapped onsite using a GPS – with the computer aided map order to see the compliance between the two, thus obtaining a measure of map-accuracy.
Yet another important reason for doing the fieldwork is that of collecting reference points to be able to geo-reference all the maps used for the project (the error in the GPS points was most of the times no more than a mere 5 meters).

3.2 Tools used during field work

A GPS of the Garmin company, "eTrex H", which was quite handy and powerful provided the most essential tool for the fieldwork.
A motorbike was also indispensible since the basin is about 30 km long and since I lived 10 km away from it.
A rubber boat was also used in order map the course of the Atankwidi river.
Figure 10 shows the GPS, the boat and the motorcycle used.

Figure 10 field work equipment, left GPS, middle boat and right the motorcycle.

3.3 The fieldwork

The fieldwork consisted of:

1) Walking around with the GPS, mapping the floodplains and agricultural features → get acquainted with the basin in general, to be able to produce a more accurate map by seeing which surfaces under which conditions give which reflections. Also necessary for the error analysis of the map, which is conducted by comparing the compliance between the GPS-mapped floodplains and the Idrisi-mapped floodplains, giving an estimate of the error.

2) Collecting reference points → to be able to better reference the images thus diminishing positional error.

3) Mapping the river course → to be able to better se the position of the river on the often blurry satellite images.

4) Keeping a journal, writing down and photographing the river depth fluctuations and changes in weather → to be able to decide which of the images are best suited for mapping and understanding the dynamics of the river.

Although no official interviews with the farmers were conducted, a great deal of spontaneous conversations was made, providing valuable information on occurrence of floods, agricultural practices, economical issues, etc.

3.4 The outcome

Unfortunately for this project – but fortunately for most of the farmers – there were no big floods in the Atankwidi basin this year (2009). Smaller floods were, however, recorded, having width of around 30 m, but given the fact that the spatial resolution of the satellite images is 12.5 meter means that this year no floods would show on the images and it will not be possible to conduct the error analysis discussed earlier in this chapter.
The trip was however not completely fruitless, a great amount of information of the flood processes and the nature of the basin itself had been acquired and all the four points pointed out in the previous chapter were conducted successfully. This information is very valuable for mapping the images of the 2007 flood and for the understanding of the flood dynamics of the basin.

4. Floodplain modeling

The floodplain modeling is conducted with the help of SOBEK and a DEM of the river basin with a resolution of 94 m.
SOBEK is developed by Delftares in collaboration with TU Delft and other dutch institutes and private consultants. SOBEK has been many time successfully used in flood simulation; e.g. in assessing the damage of dam break in Sistan-Baluchistan River Basin in Iran (Dhondia & Stelling 2002), in creating a flood hazard map using high resolution Lidar DEM (Haile & Rientjes 2004).
This chapter treats the program algorithms – i.e. explaining the way the modeling procedure is made –, the procedure behind the modeling and finally the result of the modeling.

4.1 SOBEK

The SOBEK rural module is a physical model made, amongst other, for modeling the 2D flood spread. The model is based on the calculation of the momentum and continuity equations:

- Momentum:

$$\begin{aligned} &\frac{\partial u}{\partial t} + u\frac{\partial u}{\partial x} + v\frac{\partial u}{\partial y} + g\frac{\partial \zeta}{\partial x} + g\frac{u|V|}{C^2 h} + au|u| = 0 \\ &\frac{\partial v}{\partial t} + u\frac{\partial v}{\partial x} + v\frac{\partial v}{\partial y} + g\frac{\partial \zeta}{\partial y} + g\frac{v|V|}{C^2 h} + av|v| = 0 \end{aligned} \qquad (1)$$

Where:

u	velocity in x-direction [m/s]
v	velocity in y-direction [m/s]
V	velocity: V = water level above plane of reference [m]
C	Chezy coefficient [$\sqrt{\text{m/s}}$]
d	depth below the plane of reference [m]
h	total water depth: + d [m]
a	wall friction coefficient [1/m]

- Contuniuty:

$$\frac{\partial A_f}{\partial t} + \frac{\partial Q}{\partial x} = q_{lat}$$

Where:
- A_f wetted area $[m^2]$
- q_{lat} lateral discharge per unit length $[m^2/s]$
- Q discharge $[m^3/s]$
- t time [s]
- x distance [m]

The continuity and momentum equations are solved by the Delft-Scheme which is not explained in greater detail in the SOBEK-help, stating that the Scheme operates by means of a staggered grid. In that staggered grid the water levels are defined at the connection nodes and calculation points, while the discharges are defined at the intermediate reaches or reach segments (see figure 10 below for explanaitions).

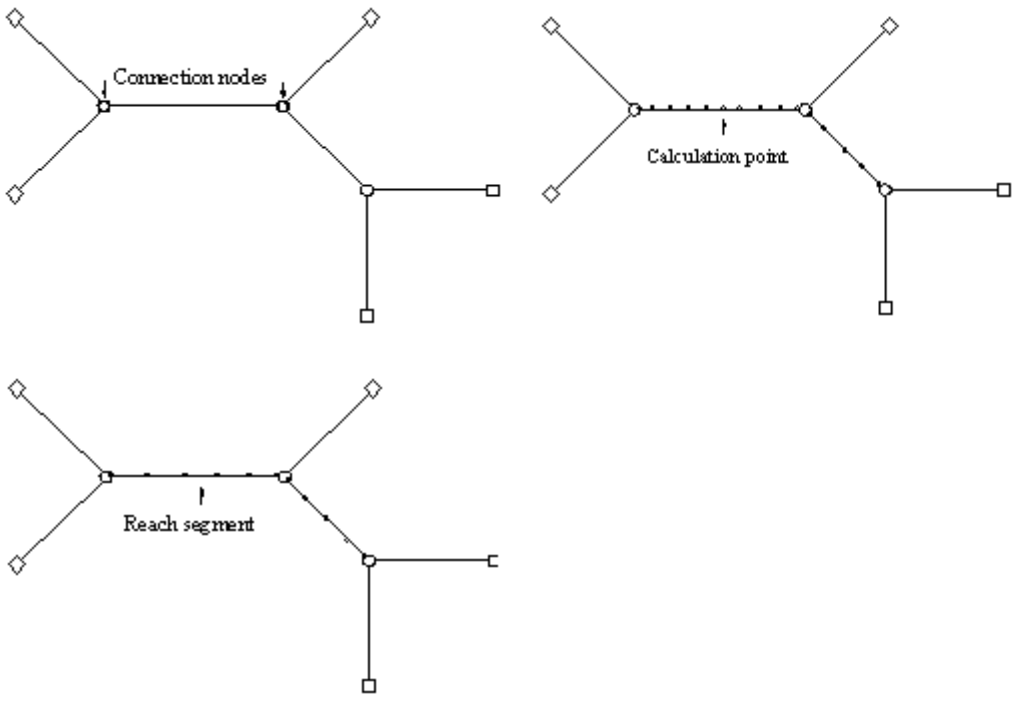

Figure 11 discription of the operation of the Delft-Scheme

4.2 The modeling

The modeling is based on solving the momentum equation over a 2D DEM grid of the Atankwidi basin.
The DEM used here where downloaded from the USGS Hydrosheds and it has a spatial resolution of 96 meters.
The schematization of the flooding was based on a simplified scheme imitating the Atankwifi River and its largest tributary (figure 12).

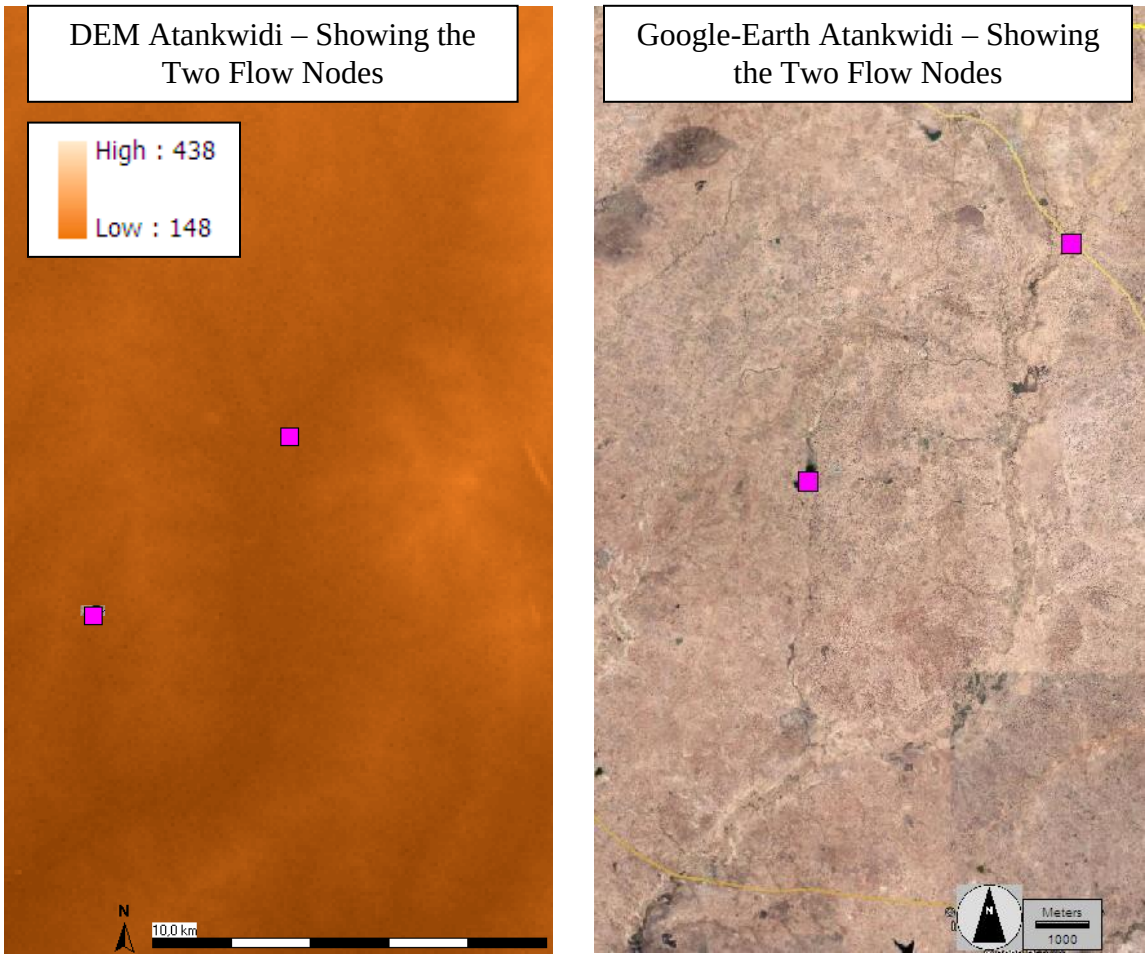

Figure 12 the simple flood model of the Atankwidi River. Coarse modeling for coarse indata. The scale in the left corner of the left images represents the elevation over sealevel (WGS).

The input into the model was the following: a flow of 200 m^3/s coming from the northern flow node and 70 m3/s coming from the southern flow node, the friction of the DEM was assigned a Manning value of 0.02 and the calculation period was 50 h (with 1h time steps). The flow values were assigned their values based on the foreknowledge of the shape and slope of the river and are a rough estimate of the maximal river discharge

during a large flood. The calculation time 50 h was enough to bring the floods to a constant level.
A more complicated schematization of the flood was tried – taking into account more of the tributaries, placing nodes on other places of the river and accounting for initial river flow – but they produced more or less the same result, demanding much longer calculation times. There is neither any need in creating a complicated schematization of the river systems because of the rough resolution of the DEM no precise results would be obtained, but only rough estimations.

4.3 Result

The modeled floodplains can be seen below in figure 13. The accuracy of the floodplains is very rough due to the rough resolution of the DEM itself – 96 m.

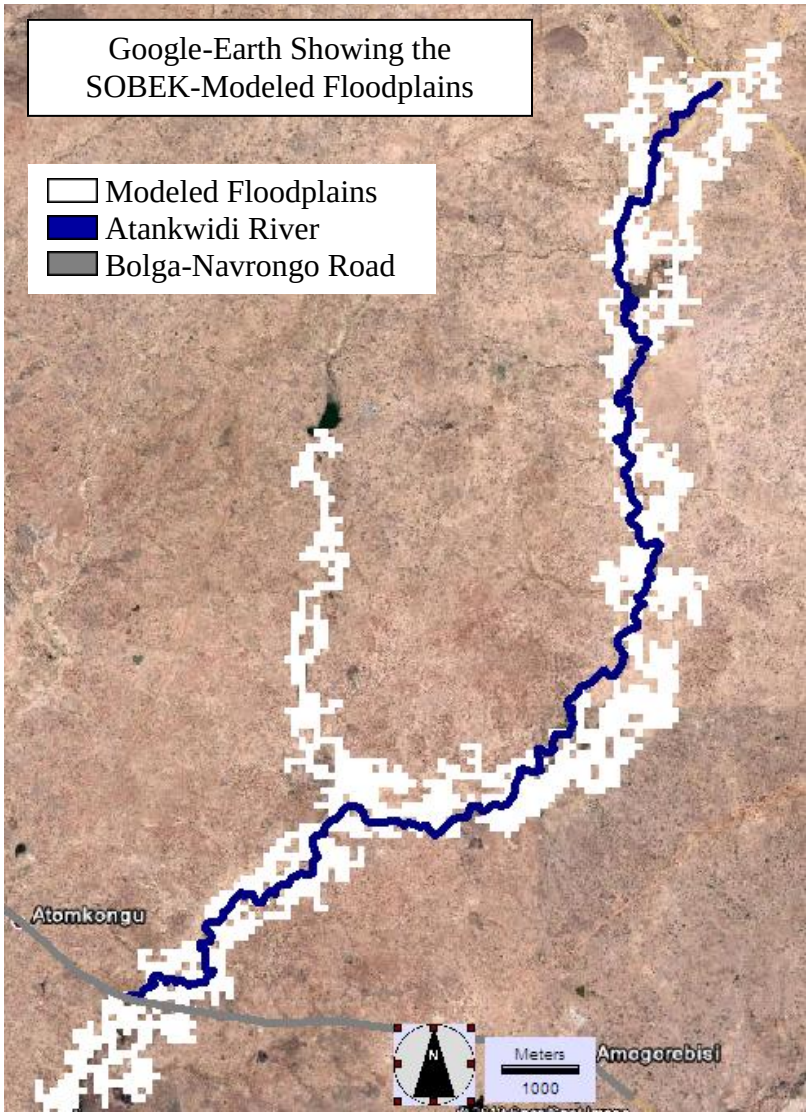

Figure 13 the modeled floodplains. Even though they look evenly distributed throughout the river course, the floodplains in the southern part of the basin stay for a much longer time because of the draining function of the basin.

One can see on the image that the areas just on the side of the river are dryer than the areas a bit farther away. This matter was discussed earlier in the chapter on the agriculture of the basin, where the millet which didn't demand a lot of water was often grown just on the river bank, while the rice – which needs a lot of water – was often grown some distance away from the Atankiwidi river. This may serve as an indication that although the resolution is rough it still manages to produce a reasonable result.

4.4 Discussion

The rough resolution of the DEM is the by far biggest obstacle in obtaining an accurate flood map. Given the fact that the Atankwidi River has a width of around 35 m and the DEM resolution is 96 m no elaborate modeling of the flooding was made with SOBEK but rather a very simplified model to show some general indications of where the floodplains could naturally be formed. Hence, the modeled floodplains do not show an exact map but more an indication of the overall flood trends in the Atankwidi Basin. The floodplains modeled are floodplains which come exclusively from the overflowing of the Atankwidi River. Much of the floodplains, especially farther away from the river, form directly from the ponded rain water.
The map should serve as good complimentary evaluation tool to the Idrisi-mapped satellite images in the following chapter.

5. Mapping C- and L-band satellite images

Satellite images of two different wave-lengths were used for the mapping of the Atankwidi River Basin, namely: L- and C-band images, with 12.5 m resolution. The mapping was made with the GIS software Idrisi.
The flood maps were only made on the 2007 flood – a map of the 2009 floodplains were to be created but due to the absence of flooding over the Atankwidi basin that year no such map could be produced.
The mapping was conducted with the help of the mapping features in idrisi and by comparing the multitemporal images of different wavelengths.

5.1 The images

The C-band images were taken from ESA's Envisat ASAR satellite. The images used had a resolution of 12.5 m.
The L-band images were taken from JAXA's Alos PALSAR satellite. The resolution of the L-band images is also about 12.5 m.
The images are covering the Atankwidi River Basin and its surroundings for the rainy and dry periods of 2007 and 2009.
The difference between the L- and the C-band images are their different wave lengths providing different type of information by highlighting differently different reflected features, thus by using the two satellites together when mapping the floodplains one can obtain a more holistic image of the real life situation.
The wavelengths of the L- and C-band radar are 15-30 cm and 4-8 cm respectively (see figure 14). For list of images used see Appendix A.

5.2 Radar

Satellite radar imagery have recently been discovered to be very useful in flood mapping (Giesen, 2001). One advantage of radar sensing as opposed to other remote sensing techniques is the ability of the radar-waves to penetrate clouds, and since the weather during floods often is cloudy this is indeed a great advantage (Liebe, 2008). Another advantage of the radar imagery is that the long waves emitted from the satellite are reflected even at low water depths. Among others, Lang (2007) has successfully used C-band images for mapping and monitoring of the forested the forested wetlands in the Mid Atlantic Region, U.S.A., monitoring as well wetlands as soil moisture.
The wavelengths of the L- and C-band radar are depicted in figure 13, putting it in perspective by comparing to other wavelengths.

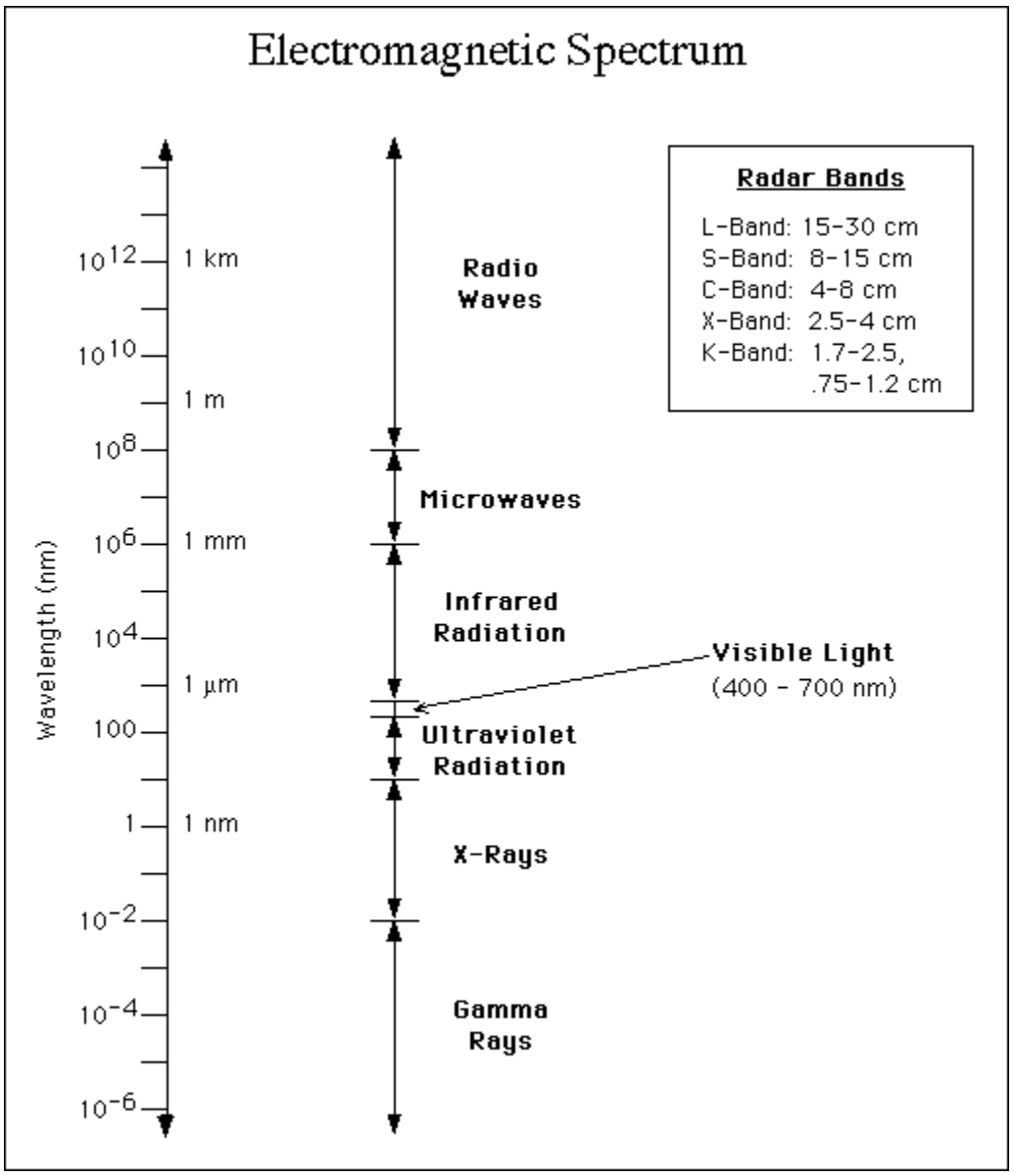

Figure 14 the electromagnetic spectrum showing the different wavelengths. (ASAR Product Handbook, 2007)

The different wavelengths give a somewhat different reflection pattern with respect to each other, thus complementing each other, making it easier to deduce more correct information.

The different scattering modes are depicted in figure 15. The reflection from water is closest to the one termed "reflection off a smooth surface". But the "double bounce" (or corner reflection) is also a common reflection from water, e.g. if the water is surrounded by high vegetation, the emitted radar signal bounces of the water surface into the surrounding vegetation returning a lot of the signal back to the sensor, producing a very bright imprint on the radar image. In his attempt on mapping the shallow floodplains in West Africa Giesen (2001) termed this enhanced reflection of water bouncing from

vegetation to "gallery forest", marking the fact of water being the underlying source of the reflection. The corner reflection from water tend to be stronger than that from a vegetated ground due to the roughness of the medium.

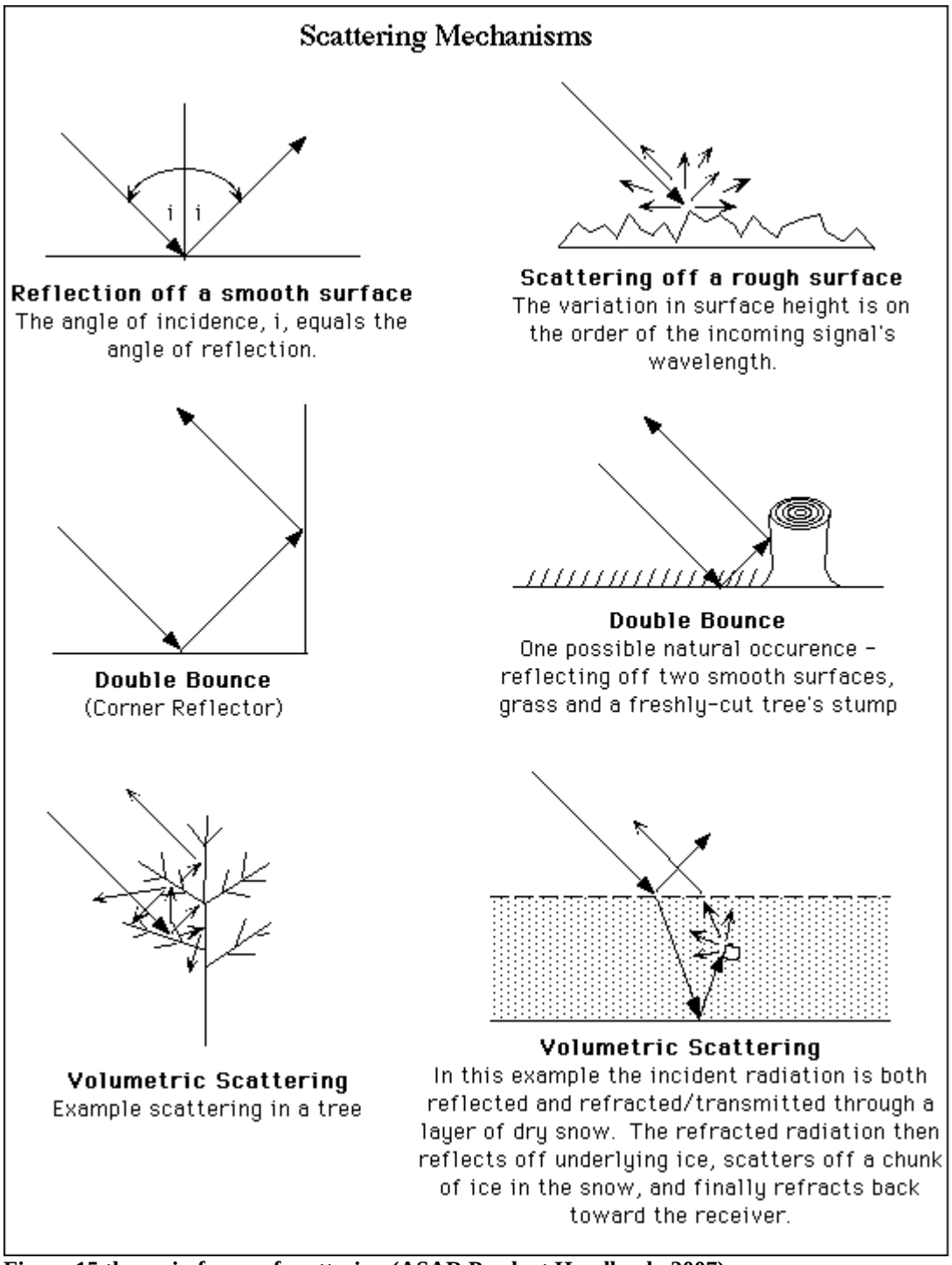

Figure 15 the main forms of scattering (ASAR Product Handbook, 2007).

5.3 Idrisi

Idrisi is a GIS software developed by Clark Labs. The software provides a powerful toolbox for image analysis by offering a range of enhancement, mapping and other analysis tools.
The software is named after the grate Andalucían cartographer of the 11th century Muhammad al-Idrisi.
The software was used for referencing, processing and mapping the L- and C-band images.

5.4 Referencing

In order to be able to compare the different images to each other they must have the same reference. The referencing was done in the following manner:

1) Referencing of the Google-Earth image using the ground-control points taken during the fieldwork in the UER. Good reference points are rigid structures like: trees, houses and junctions.

2) Using the referenced Google-Earth image to reference the rest of the images used in the analysis.

The blurriness of the satellite images made it very difficult to relate the ground-control points directly to features on the ASAR and PALSAR images. This is why the referenced Google-Earth image – and not the ground-control points – served as a reference image for the L- and C-band data.
Ground-control points, taken onsite during the fieldwork, were used for the referencing of the Google-Earth image. The accuracy of the referencing is given by Idrisi as an RMS-error which is an equivalent of the standard deviation (see equation 2).

$$RMS = \sqrt{\frac{\sum (x_i - t)}{n-1}} \qquad (2)$$

Where: $\begin{cases} x_i - measurement \\ t - true\ value \\ n - total\ number\ of\ t\ or\ x \end{cases}$

One should always strive to reduce the RMS error to less than ½ pixel-width (Eastman, 2006). The RMS was ½ pixel only for the Google-Earth image while it was around one pixel for the rest of the images, this is however still not a very problematic error-size. The RMS error for the images mapped in this report can be found in Appendix B.

5.5 Image processing

Both the C- and the L-band images came with what is termed a "salt and pepper" noise. The noise is mainly caused by mechanical or electronic interferences. Eastman (2006) states that "speckle" or "salt and pepper" noise often – especially for radar – occurs due the highly elevated reflection when the signals are reflected of edges or buildings (see "double bounce" on figure 15) which when frequent has similar effect as the "salt and pepper" noise.
In order to remove some of the noise from the images the Idrisi algorithm "Adaptive Box" was used. Eliason (1990) has proven the efficiency of the Adoptive Box in comparison with other spectral noise removing algorithms. The Adaptive Box filter is an extension of the common Lee filter and determines locally, within a specified window (3*3, 5*5, 7*7 meters), the min and max value range based on a user specified standars deviation – if the center window value is outside the user-specified range it will be considered noise and replaced by an average of its surrounding neighbors (Eastman, 2006).

5.6 The mapping algorithm

Idrisi Andes provides a multitude of different mapping functions suited for different conditions.
The mapping algorithm chosen here was the Minimum Distance algorithm. MINDIST is the most rigid mapping algorithm and fits perfectly for our case.
The MINDIST is mapping the image based in the training site data that is chosen to represent different relative features on the map. The training site data for this project consisted of four categories, namely:

1) Deeper Water
2) Flooded / Very Moist Ground
3) Gallery Forrest
4) Dry land

Those four categories were thought to be the most relevant for the project and they were also the most prevailing in the basin.
The MINDIST algorithm takes the information from the training sites and uses it for the mapping of the image. Figure 16 explains how this is done.

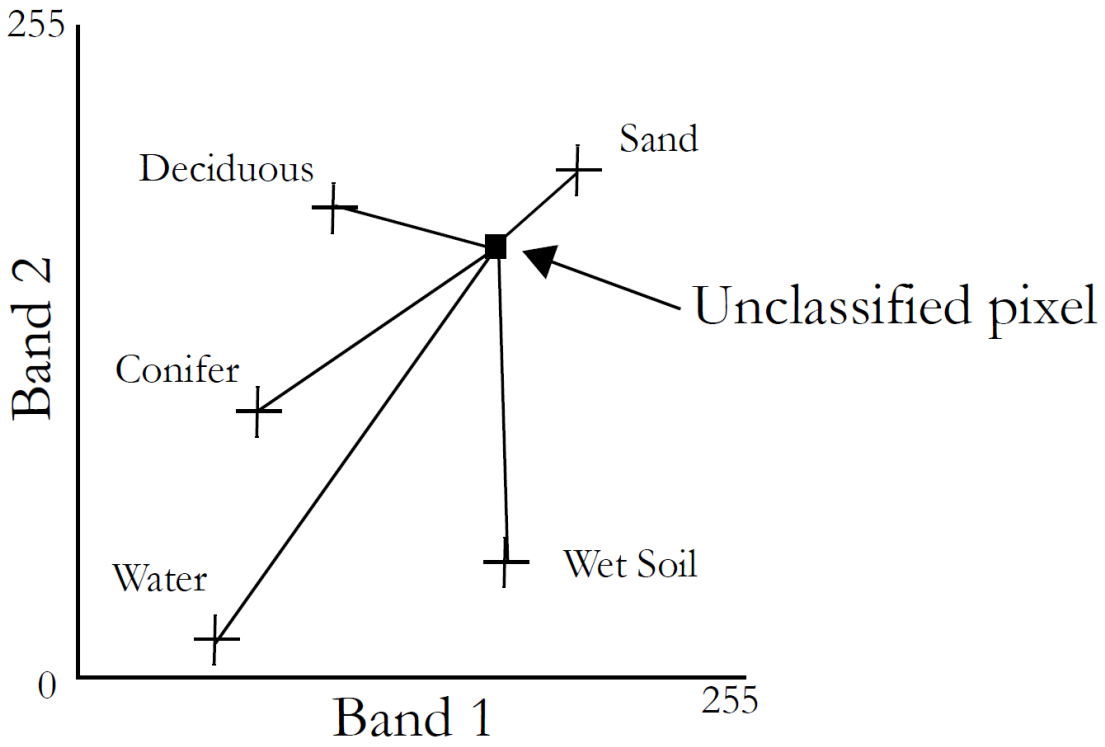

Figure 16 the mapping procedure of MINDIST (Eastman, 2006)

Hence the algorithm works just as its name implies, by finding the shortest distance from the training sites to the unclassified pixel (Eastman, 2006).

5.7 The maps

The peak of the 2007 flood is thought to have come a short time before and after the 27th of August. On the 27th of August 900 m^3/s water was released fom the Bagré Dam, drastically changing the downstream conditions for the Atankwidi River (IRIN, 2010).
The available images of the Atankwidi River Basin taken closest to the assumed flood peak were:

- (C-band) ASAR: 2007-08-26
- (L-band) PALSAR: 2007-09-04

5.7.1 PALSAR [L-band]

The L-band PALSAR radar is quite sensitive in detecting shallow water and even moist ground. This means that the light blue floodplains in figure 17 are not necessarily deep water but can also be very moist ground.
On this MINDIST mapped PALSAR image one can notice the same trend as on the flood map modeled with SOBEK, i.e. the main flooding occurs some distance away from the shores of the main river. The dark green areas are "gallery forest" they show a high reflectance on the satellite images due to the "increased reflection" phenomenon discussed in section 5.2.

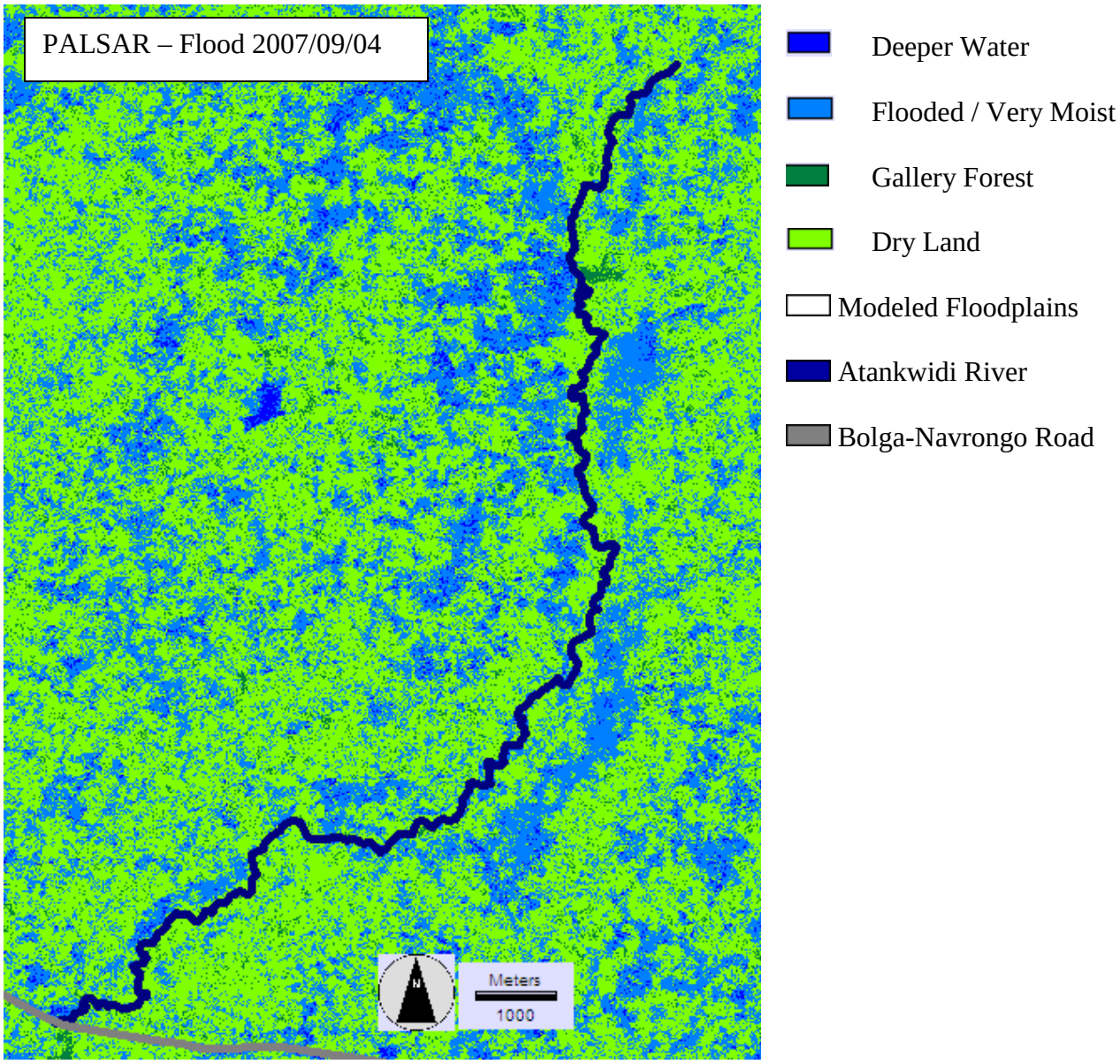

Figure 17 PALSAR-modeled floodplains of the 2007 year flood. There were no PALSAR images available for the peak days of the flood.

5.7.2 ASAR [C-band]

The ASAR image for the 2007 flood period was very noisy in its nature and very difficult to map because of the large spectral noise affecting the image. Even the Adoptive Box procedure, discussed in chapter 5.5, was not enough to bring a real order to the image and using the Adoptive Box filtering function too much takes away the much of the precision of the image. Figure 18 depicts the best try in mapping the image but there is just too much noise in the underlying ASAR images in order for us to make any real sense of the flood-map.

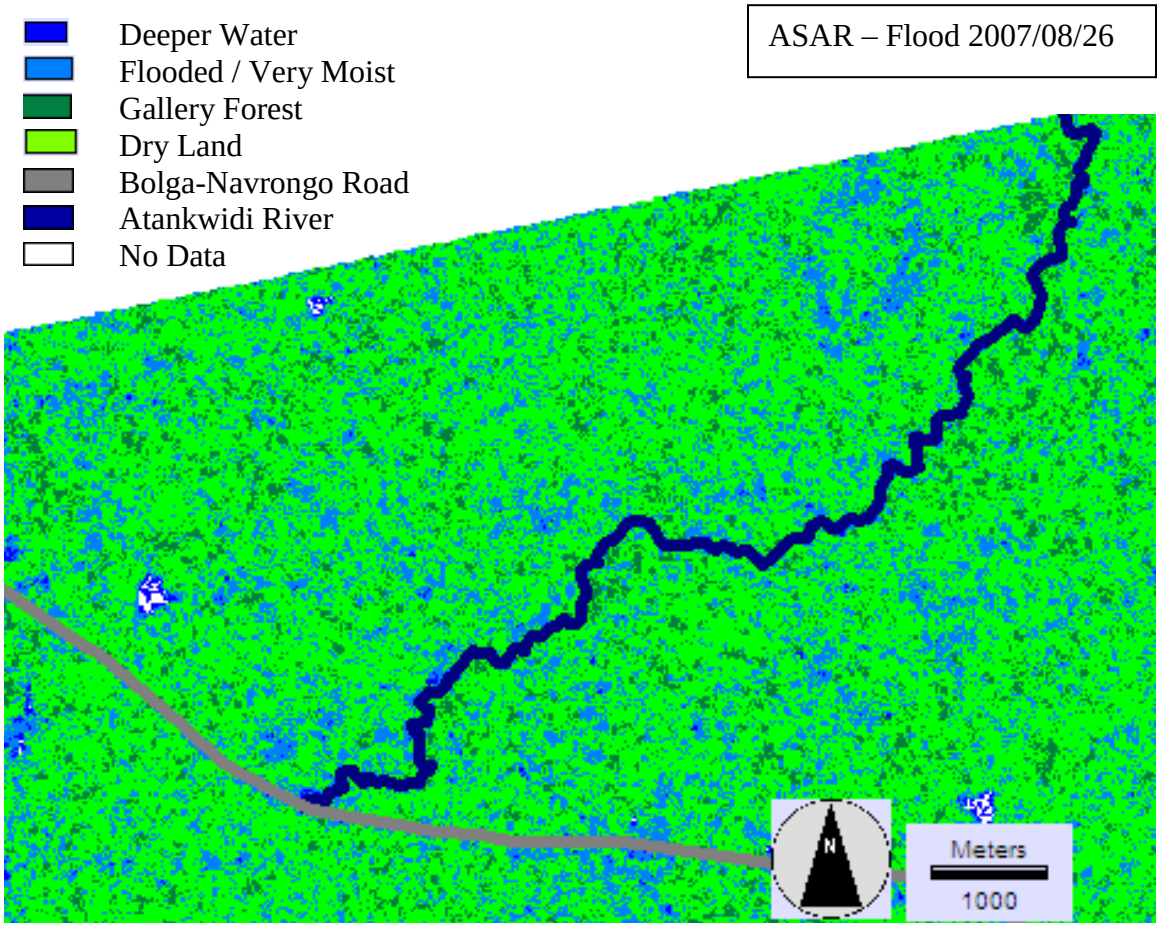

Figure 18 ASAR image taken just two days after a big rainfall with the Wite Volta downstream being flooded from the rain and Bagre Dam releases the water had nowhere to go but to pond on the surface of the saturated gound.

This noise may be due to the large flood that was over the basin at the time the image was taken. Too much corner reflection (see figure 14) may cause a high speckle noise in radar imagery (Eastman, 2006) and given that a large part of the basin was flooded high corner reflection is likely to have occurred as the radar signal bounced of the water surface and reflected of the surrounded vegetation.

5.8 Discussion

The L-band PALSAR image gives a reasonable result, showing some general floodplain areas. The floodplains, similarly to the SOBEK mapped floodplains, mostly form some distance away from the main river.
The C-band images were very noisy and it was thus difficult to collect any interesting information from them. The high spectral noise which forms the noise in the ASAR images may be due to the high corner reflection cause by the exceptionally large flood which occurred during the period.
The areas on the map that fall into the category "deep water" are those which most likely were flooded during the period, the areas which fall under the category "flooded/very moist" could – just as the name indicates – just be very shallow flood or just very moist ground, the "gallery forest" pixels are due to the double bounce phenomenon which in turn is due to the radar beam being reflected from a smooth surface and bouncing against the surrounding vegetation – this smooth surface is here thought to mostly be made up of flooded areas.

6. Comparing the SOBEK images with the satellite deduced maps

The next step in the flood analysis is to compare the Idrisi-mapped floodplains with the SOBEK-modeled ones. Here we may see if they follow the same pattern or if they differ completely.

6.1 Idrisi-PALSAR & SOBEK-DEM

Figure 19 shows the Idrisi-mapped PALSAR image next to the SOBEK-modeled DEM. The SOBEK-DEM model is very rough in resolution and is only giving a much simplified indication on how the floodplains would look like hade the river overflowed.

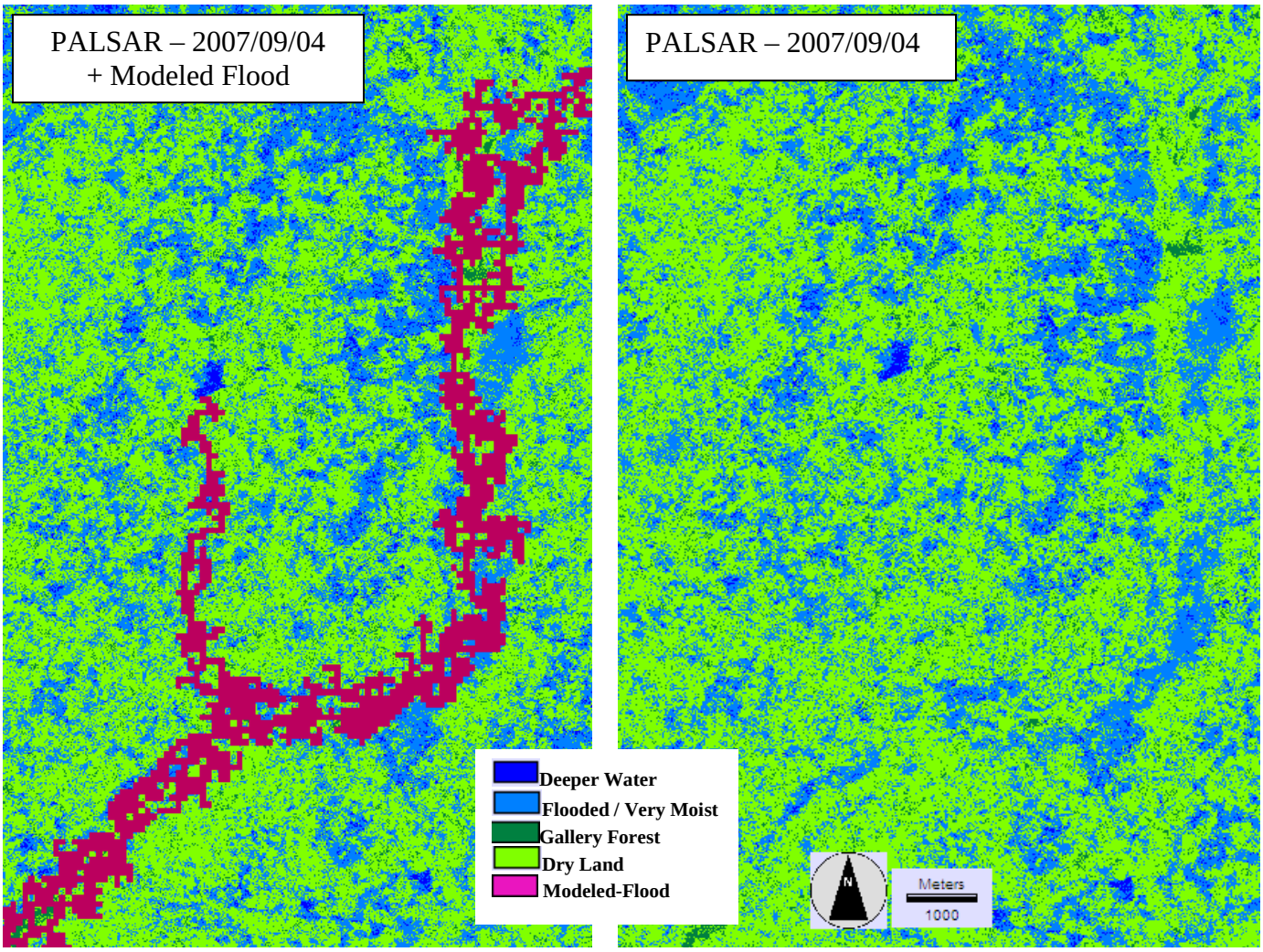

Figure 19 the PALSAR image in combination with the modeled floodplains. The floodplains follow more or less the same pattern.

One can see from the image that the two maps follow somewhat each other but the agreement is far from perfect – this again may be due to the roughness of the DEM-based map.

6.2 Idrisi-ASAR & SOBEK-DEM

Figure 20 shows the Idrisi mapped ASAR image of the 2007 flood together with the SOBEK-modeled DEM over the Atankwidi. As was discussed in the earlier chapter (5.7.2), the ASAR image was much to affected by spectral noise for it to give good information. The image was however still chosen to be shown here so that the reader can get a better visual understanding of how bad the map-accuracy was.

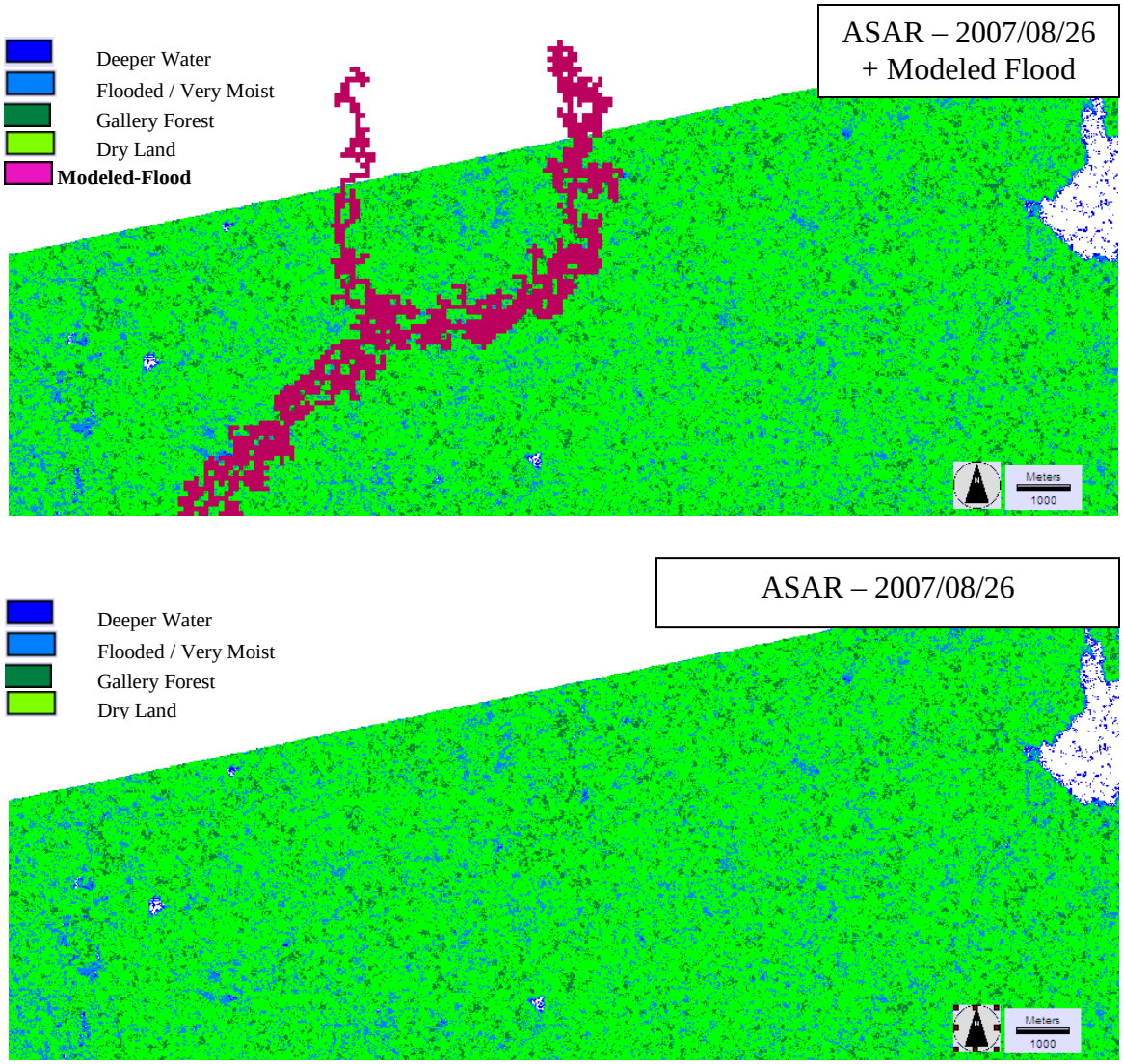

Figure 20 the asar flood image in combination with the SOBEK-modeled floodplains.

6.3 Discussion

The Idrisi-mapped PALSAR image show quite similar flood trends to the SOBEK-modeled DEM, hence complementing each other and providing basis for a more thorough analysis of the flood spread. By comparing the Idrisi-mapped image with the SOBEK-modeled image and by using the onsite experience obtained from the fieldwork it is possible to produce a qualitative flood map for 2007.
The areas which fall into the class "deep water" and are within the area of modeled floodplain are most likely to have been flooded in the 2007 flood.
The ASAR image did not give any relevant information of the flooding, this because of the large spectral-noise which made the image impossible to map, even after filtering the image several times. This noise may have been due to the large spectral reflectance from the flooded areas.

7. The Final Flood Map

This chapter is showing the final floodplain map of the areas most prone to flooding and hence the most probable floodplains during the 2007 flood. Those maps have been obtained with the help of multitemporal L- and C-band radar satellite images and a DEM of the Atankwidi river basin. The images were mapped and processed in Idrisi and the DEM was used to model the floodplains using SOBEK.
In the final step of the flood mapping both the maps produced by Idrisi and the SOBEK-modeled maps are evaluated together to mark by hand the areas most prone to flooding.

7.1 Mapping strategy

The images are, as discussed in chapter 5, divided into four categories, namely: “deeper water”, “gallery forest”, “wet ground” and “dry”. Using those four mapped classifiers together with the SOBEK-modeled map, Google-Earth and general knowledge of the area the final maps could be drawn by hand integrating all of the help-sources used.
The strategy behind the mapping is quite straight forward – mapping areas around the “deeper water” class as flooded if they are in both of the C- and L-band images taking general guidance from Google-Earth maps, the SOBEK-modeled map and ground experience.
Figure 21 on the next page shows the final “most probable” floodplain map.

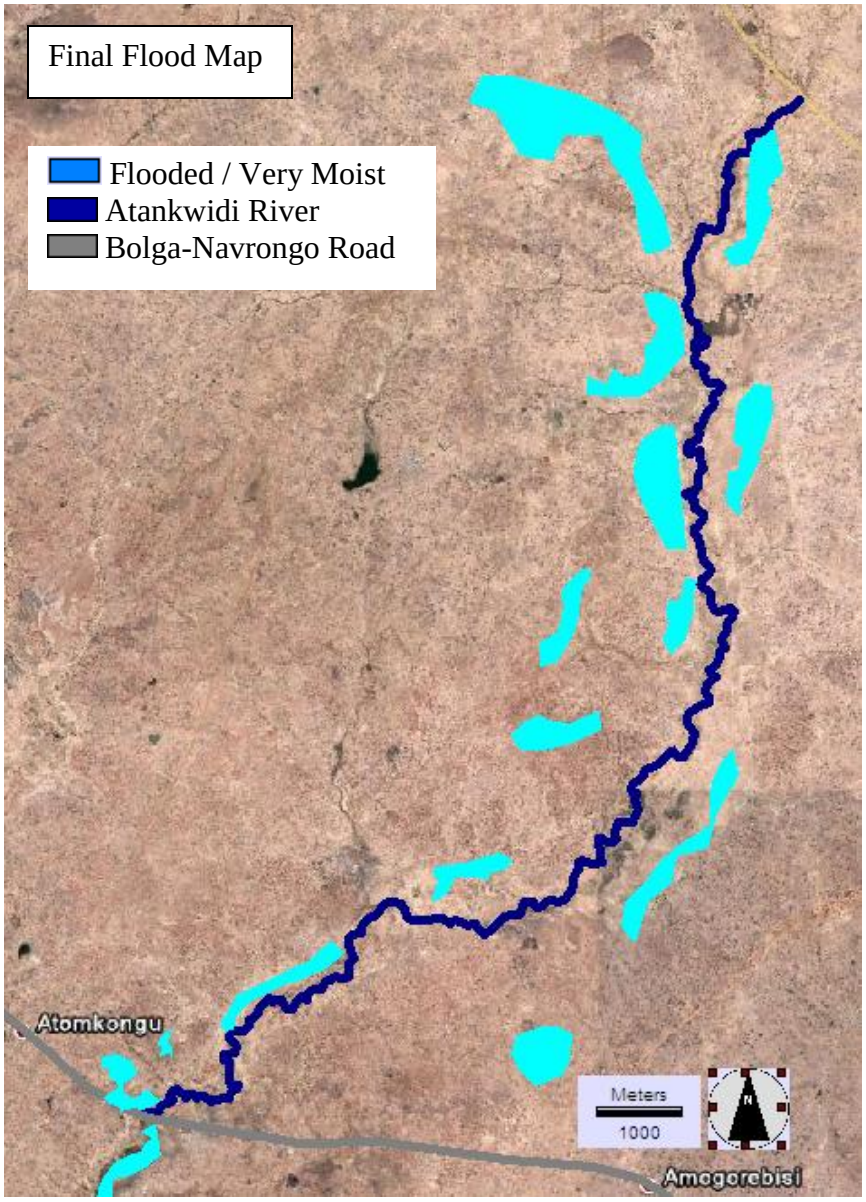

Figure 21 the final map showing an educated guess of the common locations of the floodplains in the Atankwidi River Basin

The map is only to serve as a purely indicative purpose showing the probably most common floodplains in the basin. It may serve as guidance and is nothing more than a qualitative guess.

7.2 Discussion

By comparing the mapped satellite images and the modeled DEM and using onsite experience aided by google-earth and other maps a general floodmap could be drawn, showing the largest floodplains of that particular flood.

The flood map in figure 21 is a very rough estimation of the floodplains that dominated the 2007 flood, i.e. being the largest in their extent – many more small floodplains were present, figure 16 gives much better estimation of them.

8. Discussion

Absence of larger floods during the rainy season 2009 made it impossible to map the flooding that particular year. The field work conducted in 2009 was still of vital importance as it gave the opportunity not only to familiarize myself with the basin but also to geo-reference the satellite images and the DEM.
The ASAR images proved to be too noisy for me to be able to extract any relevant information, this noise may have been due to the large flooding occurring during the time of flood, causing large spectral reflections.
The DEM used for this project had a 96m resolution which is too rough to give anything else than a rough estimate of the flood-trends. Another problem apart from the rough resolution of the DEM is that SOBEK was flooding the area by overflowing the Atankwidi River and not from precipitation, thus only producing floodplains in the absolute vicinity of the river.
The 2007 flood spread in the Atankwidi Basin is quite well depicted on the mapped PALSAR image and in combination with the SOBEK modeled floods it was possible to manually create a flood map containing the most predominant floodplains during the 2007 flood.
The result should, however, be looked upon with extreme care as the accuracy of the end product is far from precise, it is more to serve as a tool strictly for orientational purposes.
The floodplains mapped in this project can further be used to understand the shallow groundwater recharge by comparing the position of the floodplains and the position of the shallow groundwater wells dug in the basin after the 2007 flood and their yields, to verify if there indeed is a direct connection between the flood plains and the shallow groundwater yield.

Reference

Bates, P., Baldassarre, G., Schuman, G., 2009. Near Real Time Satellite Imagery to Support and Verify Timely Flood Modeling, *Wiley InterScience (www.interscience.wiley.com) DOI: 10.1002/hyp.7229*

Berg, J., 2008., Exploring Shallow Groundwater Irrigation: Current Status and Future Aplication. MSc Thesis final report. http://www.citg.tudelft.nl/live/pagina.jsp?id=d3f19bc8-7345-492d-84dd-15f8952b39dc&lang=en (TU Delft) [Accessed 27 February 2010].

Dhondia, J. F., Stelling, G. S., 2002. Application of one dimensional – two dimensional integrated hydraulic model for flood simulation and damage assessment. [Online]. Available at: http://delftsoftware.wldelft.nl/index.php?option=com_docman&task=doc_view&gid=85 (Delftares) [Accessed 03 January 2010].

Eastman, R., J., 2006., IDRISI Andes Tutorial., Clark Labs, Clark University

Eastman, R., J., 2006., IDRISI Andes Guide to GIS and Image Processing., Clark Labs, Cark University.

Eliason, E.M., McEwen, A. S., 1990. Adaptive Box Filters for Removal of Random Noise from Digital Images, *Photogrammetric Engineering and Remote Sensing*, 56(4): 453-458.

European Space Agency., 1992. *The ASAR User Guide*. [Online]: http://envisat.esa.int/handbooks/asar/CNTR.htm [Accessed January 27th 2010]

Fosu, M., 2004. Unpublished work.

Ghana High Commission., *Regions in Ghana*. [Online]: http://www.ghanahighcommissionuk.com/regions_in_ghana.php [Accessed January 26th 2010]

Giesen, N., 2001., Characterization of West African Shallow Floodplains With L- and C-Band Radar., *Remote Sensing and Hydrology, no. 267, 2001.*

Haile, T. A., Effects of LIDAR DEM resolution in flood modeling a model sensitivity study for the city of Tegucigalpa Honfuras., [Online]. Available at: http://www.commission3.isprs.org/laserscanning2005/papers/168.pdf [Accessed 03 January 2010]

IRIN, 2010. *Ghana: 'Nearly 275,000' Affected by Floods in Little-Known Disaster.* [Online]: http://www.irinnews.org/report.aspx?ReportID=74278 [Accessed January 28th 2010]

Lang, W., M., Kasischke, S., E., Prince, D., S., Pittman., W., K., 2008., Assessement of C-Band Synthetic Aperture Radar Data for Mapping and Monitoring Coastal Plain Forested Wetlands in the Mid-Atlantic Region, U.S.A., *Remote Sensing of Environment 112 (2008) 4120–4130*

Liebe, J., R., Giesen, N., Andreini, M., S., Steenhuis, T., S., Walter, M., T., 2008. *IEEE Transactions on Geoscience and Remote Sensing.*

Ross, W., 2007. *Floods Devastate Northern Ghana.*, BBC, [Online]: http://news.bbc.co.uk/2/hi/africa/6996584.stm [Accessed January 28th 2010]

Schiffer, E., McCarthy, N., Birner, R., Waale, D., Asante, F., 2008., Information Flow and Acquisition of Knowledge in Water Governance in the Upper East Region of Ghana., International Food Policy Institute.

Appendix A

Table 2 Envisat ASAR imges used for this prokect

ASAR
ASA_APP_1PNUPA***20070908***_220506_000000162061_00273_28884_2527 HV&HH
ASA_APP_1PNUPA***20070908***_220506_000000162061_00273_28884_2533 HV&HH
ASA_APP_1PNUPA***20071015***_100208_000000162062_00294_29406_2530 HV&HH – Atankwidi
ASA_APP_1PNUPA***20071013***_220503_000000162062_00273_29385_2529 HV&HH
ASA_APP_1PNUPA***20070911***_221045_000000162061_00316_28927_2534 HV&HH
ASA_APP_1PNUPA***20070911***_221045_000000162061_00316_28927_2528 HV&HH
ASA_APP_1PNUPA***20070826***_221339_000000162061_00087_28698_2526 HV&HH – Atankwidi
ASA_APP_1PNUPA***20070826***_221339_000000162061_00087_28698_2532 HV&HH – Atankwidi
ASA_APP_1PNUPA***20070823***_220757_000000162061_00044_28655_2525 HV&HH
ASA_APP_1PNUPA***20070823***_220757_000000162061_00044_28655_2531 HV&HH
ASA_IMP_1PNUPA***20070804***_220508_000000162060_00273_28383_2535 Non Polarimetric
ASA_IMP_1PNUPA***20071012***_095626_000000162062_00251_29363_2538 Non-Polarimetric
ASA_IMP_1PNUPA***20070930***_221334_000000162062_00087_29199_2537 Non-Polarimetric – Atankwidi
ASA_IMP_1PNUPA***20070923***_095336_000000162061_00480_29091_2536 Non-Polarimetric
ASA_IMP_1PNUPA***20070804***_220508_000000162060_00273_28383_2541 Non-Polarimetric
ASA_IMP_1PNUPA***20071012***_095626_000000162062_00251_29363_2544 No pol
ASA_IMP_1PNUPA***20070930***_221334_000000162062_00087_29199_2543 No pol – Atankwidi

ASA_IMP_1PNUPA***20070923***_095336_000000162061_00480_29091_2542 Non-Polarimetric
ASA_IMP_1PNUPA***20070803***_095633_000000162060_00251_28361_2540 Non-Polarimetric – Atankwidi
ASA_IMP_1PNUPA***20070803***_095633_000000162060_00251_28361_2545 Non-Polarimetric – Atankwidi
ASA_APP_1PNUPA***20090726***_221336_000000162081_00087_38718_4902 VV&HH – Atankwidi
ASA_APP_1PNUPA***20090704***_220505_000000162080_00273_38403_3045 HV&HH – Atankwidi
ASA_IM__0CNPDE***20090708***_034750_000001202080_00319_38449_3403
ASA_IM__0CNPDE***20090708***_034942_000001202080_00319_38449_3403
ASA_IM__0CNPDE***20090708***_035133_000001202080_00319_38449_3403
ASA_APP_1PNIPA***20090710***_221627_000000162080_00359_38489_2438 VV&HH
ASA_APP_1PNDPA***20090830***_221329_000000162082_00087_39219_4946 HV&HH
ASA_APP_1PNDPA***20090830***_221344_000000162082_00087_39219_4949 HV&HH – Atankwidi
ASA_APP_1PNDPA***20090918***_221618_000000162082_00359_39491_6701 HV&HH – Atankwidi
ASA_APP_1PNDPA***20090918***_221633_000000162082_00359_39491_6702 HV&HH – Atankwidi
ASA_APP_1PNUPA***20090817***_222207_000000162081_00402_39033_0467 VV&HH – Atankwidi
ASA_APP_1PNUPA***20090827***_220759_000000162082_00044_39176_3147 HV&HH – Atankwidi
ASA_APP_1PNUPA***20090902***_221913_000000162082_00130_39262_4408 VV&HH – Atankwidi
ASA_APP_1PNUPA***20090921***_222203_000000162082_00402_39534_0648 HV&HH – Atankwidi
ASA_APP_1PNUPA***20091001***_220755_000000162083_00044_39677_3513 HV&HH – Atankwidi

Table 3 PALSAR images used for this project.

PALSAR
PSR_MMC_IP__0001071001 HH&HV ***20070904***
PSR_MMC_IP__0001071002 HH&HV ***20070904*** – Atankwidi
PSR_MMC_IP__0001072001 HH&HV ***20070904***
PSR_MMC_IP__0001072002 HH&HV ***20070921***
PSR_MMC_IP__0001072003 HH&HV ***20070921***
PSR_MMC_IP__0001073001 HH&HV ***20070818***
PSR_MMC_IP__0001073002 HH&HV ***20070818***
PSR_MMC_IP__0001078001 HH&HV ***20070921***
PSR_MMC_IP__0001078002 HH&HV ***20070921***
PSR_MMC_TP__0004112001 HH&HV ***20071003***
PSR_MMC_TP__0004113001 HH&HV ***20071003***
PSR_MMC_TP__0004114001 HH&HV ***20071003***
PSR_MMC_TP__0004115001 HH&HV ***20071003***
PSR_MMC_TP__0004116001 HH&HV ***20071003***
PSR_MMC_IP__0001247001 HH ***20071020***
PSR_MMC_IP__0001247002 HH ***20071020*** – Atankwidi
PSR_MMC_IP__0001247003 HH ***20071020***
PSR_MMC_TP__0004481001 HH ***20080206***
PSR_MMC_TP__0004481002 HH ***20080206***

Appendix B

Table 4 the RMS errors of the mapped images.

Referenced Image	RMS
PALSAR 2007/09/04	17
ASAR 2007/08/26	25
Google-Earth	7